Structure–Activity Relationships of μ-Conotoxin GIIIA: Structure Determination of Active and Inactive Sodium Channel Blocker Peptides by NMR and Simulated Annealing Calculations†

Kaori Wakamatsu,*,‡ Daisuke Kohda,§ Hideki Hatanaka,§ Jean-Marc Lancelin,§ Yukisato Ishida,∥ Masanao Oya,‡ Hideshi Nakamura,⊥ Fuyuhiko Inagaki,§ and Kazuki Sato∥

Faculty of Engineering, Gunma University, Kiryu, Gunma 376, Japan, Department of Molecular Physiology, The Tokyo Metropolitan Institute of Medical Science, Bunkyo-ku, Tokyo 113, Japan, Mitsubishi Kasei Institute of Life Sciences, Machida-shi, Tokyo 194, Japan, and Department of Chemistry, Faculty of Science, Hokkaido University, Sapporo 060, Japan

Received May 28, 1992; Revised Manuscript Received September 28, 1992

ABSTRACT: A synthetic replacement study of the amino acid residues of μ-conotoxin GIIIA, a peptide blocker for muscle sodium channels, has recently shown that the conformation formed by three disulfide bridges and the molecular basicity, especially the one around the Arg[13] residue, are important for blocking activity. In the present study, we determined the three-dimensional structure of an inactive analog, [Ala[13]]μ-conotoxin GIIIA, and refined that of the native toxin by NMR spectroscopy combined with simulated annealing calculations. The atomic root-mean-square difference of the mutant from the native conotoxin was 0.62 Å for the backbone atoms (N, C^{α}, C′) of all residues except for the two terminal residues. The observation that the replacement of Arg[13] by Ala[13] does not significantly change the molecular conformation suggests that the loss of activity is not due to the conformational change but to the direct interaction of the essential Arg[13] residue with the sodium channel molecules. In the determined structure, important residues for the activity, Arg[13], Lys[16], Hyp(hydroxyproline)[17], and Arg[19], are clustered on one side of the molecule, an observation which suggests that this face of the molecule associates with the receptor site of sodium channels. The hydroxyl group of Hyp[17] is suggested to interact with the channel site with which the essential hydroxyl groups of tetrodotoxin and saxitoxin interact.

μ-Conotoxin GIIIA (previously, we called it geographutoxin I) is a sodium channel blocker peptide contained in the venomous fluid of hunting snail *Conus geographus* (Nakamura et al., 1983; Gray et al., 1988; Olivera et al., 1990, 1991). The sequence of 22 amino acid residues (Sato et al., 1983; Olivera et al., 1985) and the disulfide-bridge pairings (Hidaka et al., 1990) were determined as shown in Table I and Figure 3, respectively. This peptide blocks muscle-type sodium channels selectively (Ohizumi et al., 1986). By contrast, classical sodium channel blockers, tetrodotoxin and saxitoxin, block neuron-type sodium channels as well as muscle-type channels. In our previous synthetic studies, we found that (1) three-dimensional structures formed by three disulfide-bridges are essential for the activity, (2) the molecular basicity is important for high inhibitory activity, (3) the guanidino group of Arg[13] is the most important although not essential, and (4) two hydroxyproline residues at the sixth and seventh positions are important for correct folding of the peptide (Sato et al., 1991). We also determined the three-dimensional structure of this peptide in an aqueous solution by nuclear magnetic resonance (Lancelin et al., 1991).

For the elucidation of the structure–activity relationships of this peptide, here we determined the three-dimensional structure of an inactive analog [Ala[13]]μ-conotoxin GIIIA by NMR.[1] The native active peptide was also reanalyzed in order to compare the structures under the identical conditions. We found that the substitution of Arg[13] by Ala[13] does not

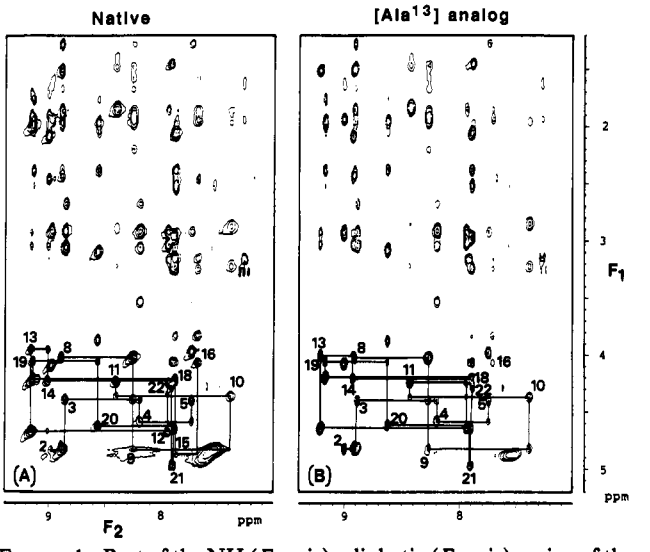

FIGURE 1: Part of the NH (F_2 axis)–aliphatic (F_1 axis) region of the NOESY spectra of (A) μ-conotoxin GIIIA and (B) [Ala[13]]μ-conotoxin GIIIA in 90% ^1H_2O/10% ^2H_2O at 400 MHz, 15 °C, and 250 ms of mixing time. Intraresidue NOESY peaks are marked with residue numbers.

† This research was partly supported by the grant from the Gunma University Foundation for Science and Technology.

* To whom correspondence should be addressed.
‡ Gunma University.
§ The Tokyo Metropolitan Institute of Medical Science.
∥ Mitsubishi Kasei Institute of Life Sciences.
⊥ Hokkaido University.

[1] Abbreviations: HPLC, high-pressure liquid chromatography; ODS, octadecylsilane; DQF-COSY, double-quantum-filtered correlation spectroscopy; E-COSY, exclusive COSY; FAB-MS, fast atom bombardment mass spectroscopy; HOHAHA, homonuclear Hartmann–Hahn spectroscopy; NMR, nuclear magnetic resonance; NOE, nuclear Overhauser effect; NOESY, NOE spectroscopy; TOCSY, total correlation spectroscopy; RMS, root mean square; RMSD, RMS difference; Hyp, *trans*-4-hydroxyproline.

0006-2960/92/0431-12577$03.00/0

Table I: Proton Chemical Shifts of μ-Conotoxin GIIIA (Upper, Roman) and of [Ala[13]]μ-Conotoxin GIIIA (Lower, Italic) at pH 3.5, 15 °C[a]

				others		
residue	NH	$C^{\alpha}H$	$C^{\beta}H$	$C^{\gamma}H$	$C^{\delta}H$	$C^{\epsilon}H$
Arg^{1}		4.10	1.95, 1.95	1.69, 1.60	3.16, 3.16	
		4.09	*1.94, 1.94*	*1.67, 1.67*	*3.16, 3.16*	
Asp^{2}	8.97	4.82	2.87, 2.87			
	9.01	*4.83*	*2.93, 2.93*			
Cys^{3}	8.85	4.42	3.06, 2.68*			
	8.89	*4.41*	*3.04, 2.69**			
Cys^{4}	8.20	4.60	3.52*, 2.92			
	8.20	*4.59*	*3.54*, 2.91*			
Thr^{5}	7.73	4.40	3.97	1.28		
	7.74	*4.40*	*3.99*	*1.28*		
Hyp^{6}		4.85	2.44, 2.01	4.69	4.14*, 3.87	
		4.83	*2.42, 2.01*	*4.69*	*4.13*, 3.87*	
Hyp^{7}		4.86	2.44, 2.36	4.63	3.73*, 3.54	
		4.84	*2.43, 2.36*	*4.63*	*3.73*, 3.54*	
Lys^{8}	8.90	4.03	2.00*, 1.88	1.52, 1.30	1.69, 1.69	3.04, 3.04
	8.91	*4.03*	*1.98*, 1.87*	*1.50, 1.29*	*1.68, 1.68*	*3.05, 3.05*
Lys^{9}	8.27	4.86	2.22, 1.93	1.58, 1.50	1.71, 1.71	3.01, 3.01
	8.28	*4.83*	*2.21, 1.92*	*1.59, 1.47*	*1.68, 1.68*	*3.04, 3.04*
Cys^{10}	7.38	4.38	3.24*, 2.86			
	7.39	*4.38*	*3.23*, 2.85*			
Lys^{11}	8.41	4.24	1.81, 1.87	1.50, 1.30	1.69, 1.69	3.00, 3.00
	8.43	*4.24*	*1.84, 1.84*	*1.48, 1.40*	*1.69, 1.69*	*2.99, 2.99*
Asp^{12}	7.94	4.64	3.00, 2.86			
	7.94	*4.64*	*3.04, 2.92*			
Arg^{13}	9.17	3.96	2.02, 1.92	1.71, 1.71	3.28, 3.28	
Ala^{13}	*9.22*	*4.01*	*1.52*			
Gln^{14}	9.02	4.24	2.09, 2.09	2.46, 2.46	NH_Z 7.68 NH_E 6.98	
	8.93	*4.22*	*2.09, 2.09*	*2.44, 2.44*	*7.69 6.98*	
Cys^{15}	7.88	4.88	3.17, 3.17			
	7.93	*4.87*	*3.18, 3.18*			
Lys^{16}	7.69	4.07	1.98, 1.87	1.58, 1.47	1.71, 1.71	2.95, 2.95
	7.71	*4.06*	*1.95, 1.86*	*1.59, 1.49*	*1.69, 1.69*	*2.94, 2.94*
Hyp^{17}		4.67	2.42, 1.99	4.52	3.85*, 3.25	
		4.66	*2.41, 1.97*	*4.50*	*3.84*, 3.25*	
Gln^{18}	7.89	4.22	2.07, 2.07	2.53, 2.39	NH_Z 7.54 NH_E 7.07	
	7.90	*4.21*	*2.07, 2.07*	*2.53, 2.39*	*7.57 7.08*	
Arg^{19}	9.15	4.07	1.97, 1.97	1.76, 1.76	3.27, 3.27	
	9.18	*4.06*	*1.98, 1.98*	*1.78, 1.78*	*3.26, 3.26*	
Cys^{20}	8.57	4.64	3.89, 3.10*			
	8.63	*4.62*	*3.88, 3.09**			
Cys^{21}	7.89	4.99	3.24*, 2.98			
	7.90	*4.99*	*3.24*, 2.99*			
Ala^{22}	7.92	4.29	1.46			
	7.89	*4.29*	*1.45*			
$CONH_Z$	7.61	$CONH_E$	7.11			
	7.63		*7.12*			

[a] An asterisk indicates the $H^{\beta 3}$ ($H^{\delta 3}$) proton when the $C^{\beta}H$ ($C^{\delta}H$) methylene have been stereospecifically assigned. H_Z and H_E refer to NH protons cis and trans to C^{γ} (C^{α} for Ala^{22}), respectively.

significantly change the molecular conformation. This suggested that the Arg^{13} residue is directly involved in the binding to sodium channel molecules. Considering the effects of various amino acid substitutions on the activity on the basis of the three-dimensional structure of the toxin, we postulate the binding topology of this toxin to the sodium channel molecule. Similarities with classical low-molecular-weight sodium channel blockers are also discussed.

EXPERIMENTAL PROCEDURES

Materials. μ-Conotoxin GIIIA and [Ala^{13}]μ-conotoxin GIIIA were synthesized in a large quantity by the same strategy as described previously (Sato et al., 1991). Primary structures and the purities of synthetic peptides were confirmed by analytical HPLC, amino acid analysis, and FAB-MS measurement.

NMR Measurements. All NMR spectra were recorded on Bruker AM-400 and AM-500 spectrometers operating at 400 and 500 MHz, respectively. Peptides were dissolved in 99.98% ^2H_2O or 90% ^1H_2O/10% ^2H_2O at 20 mM concentration. No symptom of self-aggregation was detected such as a concentration dependence of chemical shifts. The sample pH was adjusted to 3.5 with HCl (direct pH meter reading) in order to decrease the exchange rates of amide protons with solvent.

Table II: Structural Statistics[a]

	native		Ala[13] analog	
	10 structures	mean structure	10 structures	mean structure
RMS deviations from experimental distance restraints[b]	0.080 ± 0.002 (91)	0.08	0.049 ± 0.003 (87)	0.046
RMS deviations from experimental dihedral angle restrains	3.1 ± 0.6 (20)		1.2 ± 0.5 (19)	
F_{NOE} (kcal·mol^{-1})[c]	29.4 ± 1.5	29.4	10.3 ± 1.3	9.09
F_{tor} (kcal·mol^{-1})	3.0 ± 1.2	2.4	0.50 ± 0.40	0.0
F_{repel} (kcal·mol^{-1})	19.1 ± 1.4	14.6	17.2 ± 1.2	16.2
F_{total} (kcal·mol^{-1})[d]	433.0 ± 6.4	1049.3	385.3 ± 3.4	1013.3
$E_{L\text{-}J}$ (kcal·mol^{-1})[e]	−76.8 ± 6.7	−78.7	−75.2 ± 4.2	−66.5
RMS deviations from idealized geometry				
bonds (Å)	0.005 ± 0.001 (357)	0.005	0.0046 ± 0.0005 (343)	0.004
angles (deg)	1.87 ± 0.01 (653)	3.12	1.852 ± 0.007 (629)	3.17
impropers (deg)[f]	1.12 ± 0.02 (115)	1.09	1.14 ± 0.01 (109)	1.14

[a] The "10 structures" refers to the 10 annealed structures having the smallest F_{total} value; the "mean structures" refers to the restrained minimized structure obtained by restrained minimization of the averaged coordinates of the individual 10 structures; the number of constraints is given in parentheses. [b] No structures have distance violation greater than 0.4 Å. [c] The values of the force constants used for the calculation of the square-well potentials are the original values of 50 kcal·mol^{-1}·Å^{-1} and 200 kcal·mol^{-1}·rad^{-2}, for NOE and torsion angle potentials, respectively. The value of the van der Waals repulsion term is calculated with the original force constant of 4 kcal·mol^{-1}·Å^{-4} with the van der Waals radii scaled by a factor 0.8 times the standard value used in the CHARMM empirical function (Brooks et al., 1983). [d] F_{total} is the sum of F_{NOE}, F_{tor}, F_{repel}. [e] $E_{L\text{-}J}$ is the Lennard-Jones van der Waals energy calculated with the CHARMM empirical energy function (Brooks et al., 1983), which was not included in the simulated annealing calculation. [f] The improper torsion terms are used to maintain the planar geometry as well as the chiralities.

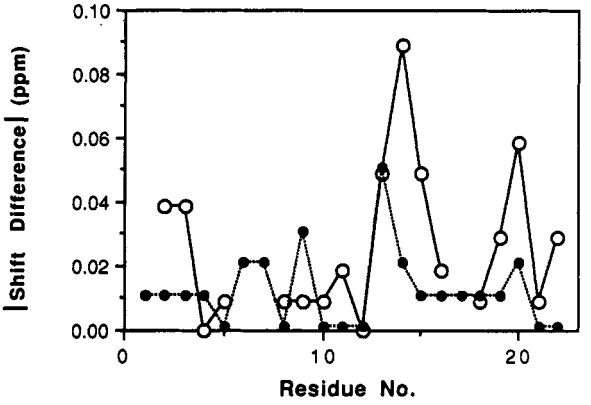

FIGURE 2: Chemical shift differences of [Ala[13]]μ-conotoxin GIIIA from μ-conotoxin GIIIA (absolute value). Open and filled circles indicate the shift difference of NH and C$^{\alpha}$H, respectively.

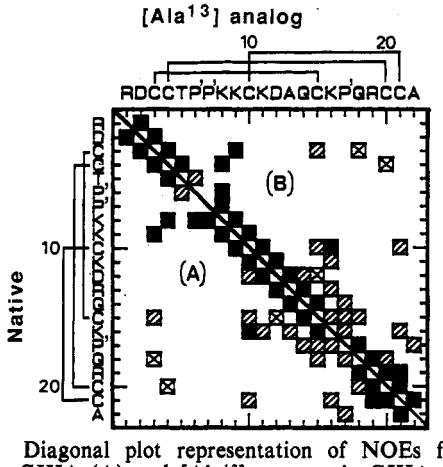

FIGURE 3: Diagonal plot representation of NOEs found for μ-conotoxin GIIIA (A) and [Ala[13]]μ-conotoxin GIIIA (B). The squares connect the pairs of the amino acids for which NOEs were observed. The filled squares, hatched squares, and crossed squares indicate main-chain–main-chain, main-chain–side-chain, and side-chain–side-chain NOEs, respectively.

Although side chains of two aspartic acid residues are somewhat protonated at this pH, our previous substitution study showed that the negative charges at these residues do not contribute to the activity of the toxin molecule (Sato et al., 1991). The temperature was set to 15 °C for NOESY and to 30 °C for other two-dimensional measurements. Two-dimensional DQF-COSY (Rance et al., 1983), TOCSY/HOHAHA (Bax & Davis, 1985), E-COSY (Griesinger et al., 1985), and NOESY (Jeener et al., 1979; Macura et al., 1981) spectra were recorded in a phase-sensitive mode (Bodenhausen et al., 1984). The mixing times of NOESY experiments were 100, 200, 250, and 300 ms. The water resonance was suppressed by preirradiation (DQF-COSY and TOCSY) or a jump-and-return (Plateau & Guéron, 1982) read pulse (NOESY). Spectral width in both dimensions was 5000 Hz for 90% ^1H_2O sample and 3000 Hz for ^2H_2O sample. Time domain data points were 4096 (t_2) × 1024 (t_1) for E-COSY and 2048 (t_2) × 512 (t_1) for other measurements. Frequency domain data points were 4096 (f_2) × 2048 (f_1) for E-COSY and 2048 (f_2) × 1024 (f_1) for other measurements. Before Fourier transformation, time domain data were multiplied by a squared sine bell function with a $\pi/4$ phase shift in both dimensions.

Computing Procedures. Energy minimization and simulated annealing calculations were made with the program XPLOR (version 2.1, Polygen Corp., Waltham, MA) on a Personal Iris 35 workstation (Silicon Graphics Inc., Mountain View, CA). Initial structures were generated using random ϕ and ψ angles with side chains in an extended conformation and perfect covalent geometry. ω angles were set to trans except for the Hyp7 ω, the value of which was set to the cis configuration (Lancelin et al., 1991). For simulated annealing calculations, the YASAP protocol of XPLOR was used (Nilges et al., 1988; Brünger et al., 1990). The target function to be minimized has the form

$$F_{total} = F_{bond} + F_{angle} + F_{impr} + F_{repel} + F_{NOE} + F_{tor}$$

where F_{bond} and F_{angle} describe the covalent energy terms for maintaining correct bond lengths and bond angles, respectively. F_{impr} describes energy involving chirality and planarity. F_{repel} describes a repulsion term for preventing unduly close contacts of atoms. F_{NOE} and F_{tor} describe square-well potentials for introducing penalties when the interproton distances or torsion angles deviate from the acceptable value ranges which were determined experimentally. A detailed definition is given by Clore et al. (1986).

The interproton distances involving methylene protons without stereospecific assignments were referred to single

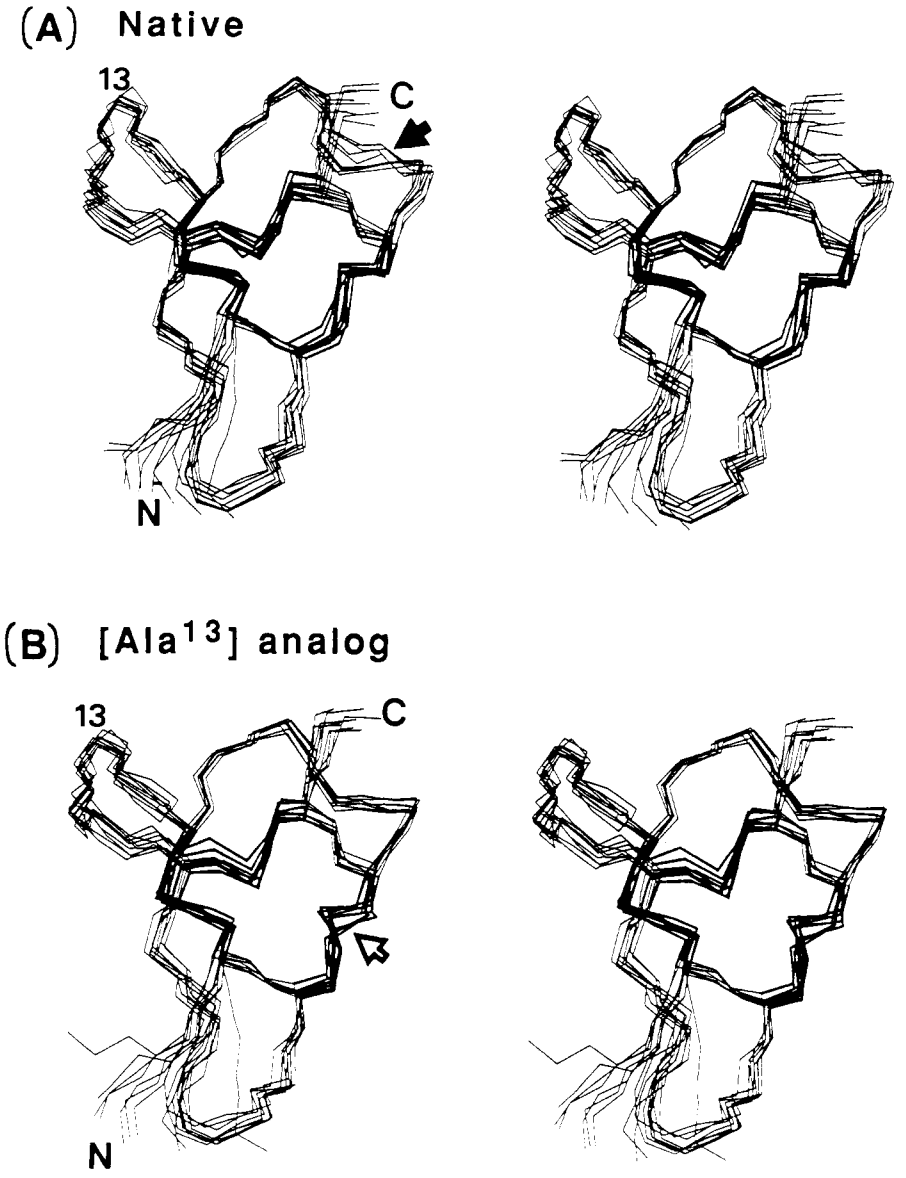

FIGURE 4: Stereopair of the best-fit superposition of the 10 converged structures of (A) μ-conotoxin GIIIA and (B) [Ala[13]]μ-conotoxin GIIIA. In addition to the (N, C^{α}, C′) backbone atoms, C^{β}, C^{γ}, and C^{δ} of Hyp are displayed with C^{β} and sulfur atoms of Cys in bold lines. Less defined structures in the native peptide and in the analog peptide are marked with a filled and an empty arrow, respectively.

Table III: Atomic RMS Differences between 10 Structures and Mean Structures of Native Peptide and [Ala[13]]Peptide (Å)[a]

			RMSDs (Å) (residue number)	
	structure	fitted to	2–21	2–10, 14–21
N,C^{α},C′	CTX	CTX mean	0.48 ± 0.11	0.48 ± 0.10
	R13A	R13A mean	0.45 ± 0.12	0.44 ± 0.14
	CTX	R13A mean	0.72 ± 0.14	
	R13A	CTX mean	0.67 ± 0.12	
	CTX mean	R13A mean	0.62	
all heavy atoms	CTX	CTX mean	1.18 ± 0.15	1.06 ± 0.18
	R13A	R13A mean	1.10 ± 0.08	1.06 ± 0.09
	CTX	R13A mean	1.37 ± 0.22	
	R13A	CTX mean	1.37 ± 0.16	
	CTX mean	R13A mean	1.06	

[a] CTX and R13A refer to μ-conotoxin GIIIA and [Ala[13]]μ-conotoxin GIIIA, respectively.

$(\langle r^{-6} \rangle)^{-1/6}$ average distances so that no corrections for pseudoatom treatments were made. An electrostatic term, a 6–12 Lennard-Jones term, or hydrogen bonds were not taken into account in the present structure calculation.

Analyses of the Calculated Structures. Analyses of structures were carried out with XPLOR-UP (XPLOR utility programs, Kohda et al., unpublished results), and displaying and plotting of structures were carried out with QUANTA (version 3.2, Polygen Corp., Waltham, MA) on an Iris 4D/70G. For a quantitative assessment of the convergence of the calculations, a partial sum, $F_3 = F_{repel} + F_{NOE} + F_{tor}$ was computed for each structure. Ten annealed structures with the smallest F_3 values were selected for each peptide. For quantitative comparisons of different structures, minimum RMS differences (RMSDs) were calculated for the backbone atoms (N, C^{α}, C′) of residues 2–21. A mean structure was obtained for each peptide by averaging the coordinates of the structures that had been superimposed in advance on the best converged structure. Because such an averaged structure was poor in geometry, mean structures were subjected to a restrained Powell minimization: 200 cycles with the soft van der Waals radii reduced by a factor of $s = 0.25$, 200 cycles with $s = 0.5$, and 800 cycles with $s = 0.8$ (Clore et al., 1986). The final coordinates of each annealed structure were obtained by fitting them to the mean structure for the backbone atoms of residues 2–21. RMSDs per residue were calculated between

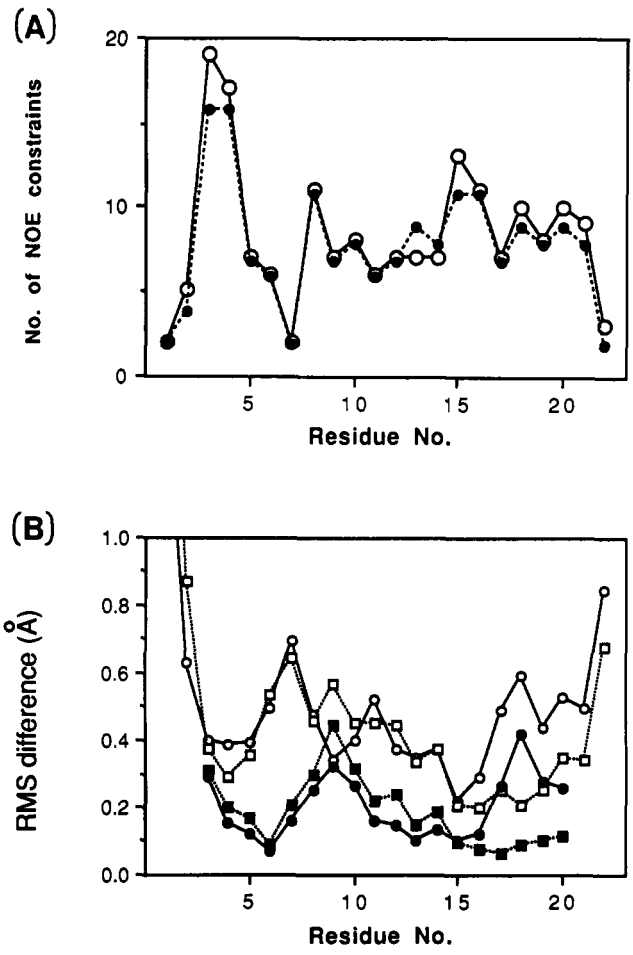

FIGURE 5: Distribution along the amino acid sequences of (A) the number of distance constraints for μ-conotoxin GIIIA (empty circles) and for [Ala[13]]μ-conotoxin GIIIA (filled circles). (B) atomic RMS difference from the mean structure per residue calculated without (empty symbols) or with a five-residue window (filled symbols) for μ-conotoxin GIIIA (circles) and [Ala[13]]μ-conotoxin GIIIA (squares).

the individual final structures and their mean structure.

RESULTS

Resonance Assignment. The resonance assignments of μ-conotoxin GIIIA have been published (Lancelin et al., 1991). But because there are some differences in the experimental conditions, sequence-specific assignments of proton resonances of the native peptide as well as the Ala[13] analog were carried out independently in this study. This was done by the conventional method (Wüthrich, 1986). Aliphatic proton (F_1)/amide proton (F_2) regions of NOESY spectra in Figure 1 depict connectivities of the spin systems of the two peptides. Proton resonance assignments of two peptides are listed in Table I. Chemical shift changes of backbone protons (NH and $C^\alpha H$) accompanied by the substitution from Arg[13] to Ala[13] are small (≤0.10 ppm) as shown in Figure 2, suggesting that the backbone conformation of the peptide does not change largely upon the substitution. Diagonal plots of the two peptides are nearly identical as shown in Figure 3. Although there are successive medium-range NOEs between the ith residue and the (i+3)th residue in the Asp[12]–Gln[18] segment, this segment is not in the typical α-helical conformation since NOE cross peaks between proton pairs such as $C^\alpha H(i)$–$C^\beta H$-(i+3) and $C^\alpha H(i)$–NH(i+3) were not observed.

Input Data for the Three-Dimensional Structure Calculations. Stereospecific assignments of nonequivalent C^β protons were done by referring to intraresidue NOEs of $C^\alpha H$–$C^\beta H$ and NH–$C^\beta H$, and to the $^3J_{\alpha-\beta}$ coupling constants determined by E-COSY experiments according to Wagner et al. (spectra not shown). At the same time, ranges of χ_1 angles were determined for residues Cys[3], Cys[4], Lys[8], Cys[10], Cys[20], and Cys[21] for both peptides. We used as input data for structure calculations 62 (56) sequential and 40 (42) long-range NOEs for the native peptide. (The numbers in the parentheses are the corresponding values for the Ala[13] analog.) These NOEs were classified into three distance constraints: ≤2.5, ≤3.0 and ≤4.0 Å, corresponding to the strong, medium, and weak intensity of NOESY cross peaks at 15 °C and 250 ms of mixing time. At this mixing time, spin diffusion effects were not observed both in this study and in the previous study (Lancelin et al., 1991). The NOE data were converted to 91 (87) final distance constraints. Fourteen (13) constraints on the angle ϕ and 6 (6) on the angle χ_1 were also introduced according to the following rules (Wagner et al., 1987): a $^3J_{HN\alpha}$ greater than 8 Hz contrained the ϕ angle in the range of $-120 \pm 40°$; a $^3J_{HN\alpha}$ less than 5 Hz constrained the ϕ angle in the range of $-65 \pm 25°$. A t^2g^3 side-chain conformation constrained the χ_1 angle in the $-60 \pm 60°$ and a g^2g^3 in the $60 \pm 40°$ range. Disulfide bridges between Cys[3] and Cys[15], Cys[4] and Cys[20], and Cys[10] and Cys[21] put constraints between sulfur atoms S(i)–S(j) as 2.02 ± 0.10 Å. No additional distance constraints were introduced such as slowly exchanging amide proton information (hydrogen bonding) or intraresidue NOEs. Input data for structure calculations are available in the supplementary material.

Structure Calculations. We made preliminary computations of 100 solution structures for each peptide in order to evaluate the folding of the main chain and the overall consistency of our input data sets. In the 20 structures with the smallest F_3 values, one distance constraint between $C^\alpha H$ of Thr[5] and $C^\gamma H$ of Hyp[7], which had a systematic violation of more than 0.5 Å, was eliminated. After this modification, we computed 200 solution structures for both peptides. We selected 10 structures for both peptides as described under Experimental Procedures. Structural statistics for the final structures are listed in Table II.

Description of Tertiary Structures. Figure 4 panels A and B show the best-fit overlays of the 10 converged structures of μ-conotoxin GIIIA and of [Ala[13]]μ-conotoxin GIIIA, respectively. The folding of the peptide backbone is the same as that obtained previously (Ott et al., 1991; Lancelin et al., 1991). Atomic RMSDs for each peptide are summarized in Table III. The convergence of structures for the two peptides does not differ significantly.

In Figure 5B are plotted atomic RMSD values from the mean structure along the amino acid sequence. Larger RMSD values of the native peptide than those of Ala[13] analog in the Hyp[17]–Gln[18]–Lys[19] segment are not due to the real structural disorder in this segment but to an artifact in the calculation. When ϕ–ψ pairs of the 10 calculated structures are plotted for each residue, the ϕ–ψ pairs in the Hyp[17]–Gln[18]–Lys[19] segment are distributed in two clusters in the case of the native peptide (data not shown). In the case of the Ala[13] analog, however, ϕ–ψ pairs are distributed in only one cluster which corresponds to the one of the two clusters in the case of the native peptide (data not shown). The apparent disorder in the Hyp[17]–Gln[18]–Lys[19] segment is recognized in Figure 4A (filled arrow). On the other hand, the disulfide structure of Cys[4]–Cys[20] of the Ala[13] analog is less-defined and shows a mirror image (Figure 4B; empty arrow). The corresponding disulfide structure of the native peptide is well-defined. Thus the structures in the two segments (the Hyp[17]–Gln[18]–Lys[19]

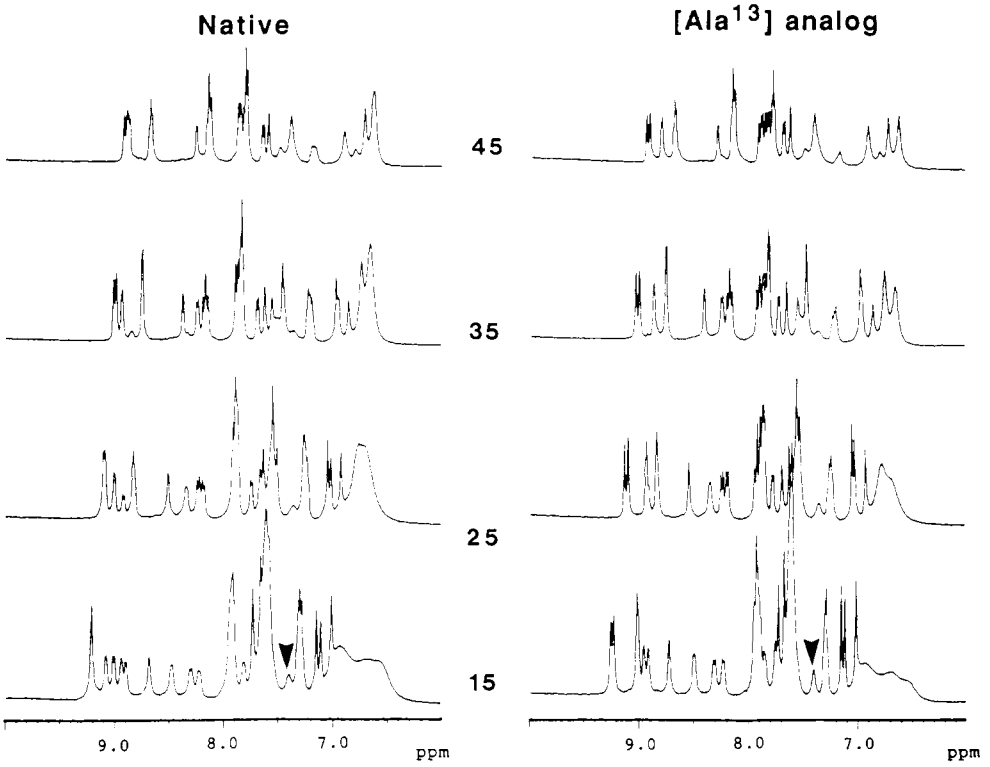

FIGURE 6: Amide proton region of the ^{1}H NMR spectra of μ-conotoxin GIIIA (left stack) and of [Ala^{13}]μ-conotoxin GIIIA (right stack) at 15, 25, 35, and 45 °C. Amide proton resonances of Cys^{10} are marked with arrowheads.

segment and the Cys^4–Cys^{20} disulfide bridge) seem to affect each other during the simulated annealing calculations. When RMSD values per residue are calculated by fitting all residues except the terminal residues to the mean structure, the Hyp^6–Hyp^7–Lys^8 segment appears slightly less defined as well as the two terminal segments for both peptides.

But when the RMSD values per residue are calculated by fitting the local five residues of each structure to the corresponding five residues of the mean structure (i.e., with a five-residue window), the high values of the Thr^5–Hyp^6–Hyp^7 segment decreased. Interestingly, the Lys^8–Lys^9–Cys^{10} segments of the two peptides were left as the most disordered region.

DISCUSSION

Description of the Calculated Structure. To make it clear whether the Arg^{13} residue of μ-conotoxin GIIIA interacts directly with sodium channel molecules or this residue is important for maintaining the correct folding of the toxin, we determined the three-dimensional structure of the inactive analog [Ala^{13}]μ-conotoxin GIIIA in an aqueous solution in detail. We also reanalyzed the structure of active peptide μ-conotoxin GIIIA to compare the structures under the identical conditions. The structure obtained for the latter is very similar to those previously reported by Ott et al. (1991) and Lancelin et al. (1991). However, the convergence of the structures in the present study is better than those previously published, because of the larger number of constraints on both interproton distances and ϕ angles and because of a new simulated annealing program used (YASAP).

We previously reported that the Lys^{11}–Arg^{13} segment is less defined (RMSD value of ca. 1.5 Å) than the rest of the molecule [RMSD value of ca. 0.7 Å; refer to Figure 10 of Lancelin et al. (1991)]. This observation was not reproduced in the present calculations (Figure 5B). In agreement with this, the value of atomic RMS difference versus mean structure does not decrease significantly when the Lys^{11}–Arg^{13} segment is excluded in fitting (Table III). The difference in the degree of convergence for the Lys^{11}–Arg^{13} segment is not due to the difference in the distribution of the distance constraints over the sequence [compare Figure 5A with Figure 10a of Lancelin et al. (1991)] but is ascribed to the different simulated annealing programs used, since the input data used previously (Lancelin et al., 1991) gave uniformly converged structures when processed with the new version of the program, YASAP (data not shown). A different structure calculation program DSPACE (Hare Research, Inc., Bothwell, WA) also gave converged structures for the segment Lys^{11}–Arg^{13}, in agreement with the data obtained with YASAP. We previously suggested a possible connection between the important Arg^{13} and the "flexibility" of the segment containing Arg^{13}, but this must be reconsidered.

The amide proton of Cys^{10} exhibits anomalous behavior; it becomes broader as temperature increases (Figure 6). The broadening of the resonance upon raising the temperature is probably due to the chemical exchange of the proton between two or more different states. Atomic RMSD values are considerably smaller when calculated with a five-residue window than when calculated without the window. The Lys^8–Lys^9–Cys^{10} segment shows high RMSD values even with the five-residue window, however, which supports the chemical exchange. Previously, we regarded this anomalous behavior of Cys^{10} NH as the support for the segmental motion of the Lys^{11}–Arg^{13} portion (Lancelin et al., 1991). This behavior is also found after the replacement of Arg^{13} residue by Ala^{13} residue (Figure 6).

Comparison of the Two Structures. The backbones of the mean structures of the native peptide and Ala^{13} analog are superimposed in Figure 7. Main-chain foldings of the two peptides are essentially identical.

To allocate the part which takes a different conformation between the two structures, if any, atomic RMSD values are

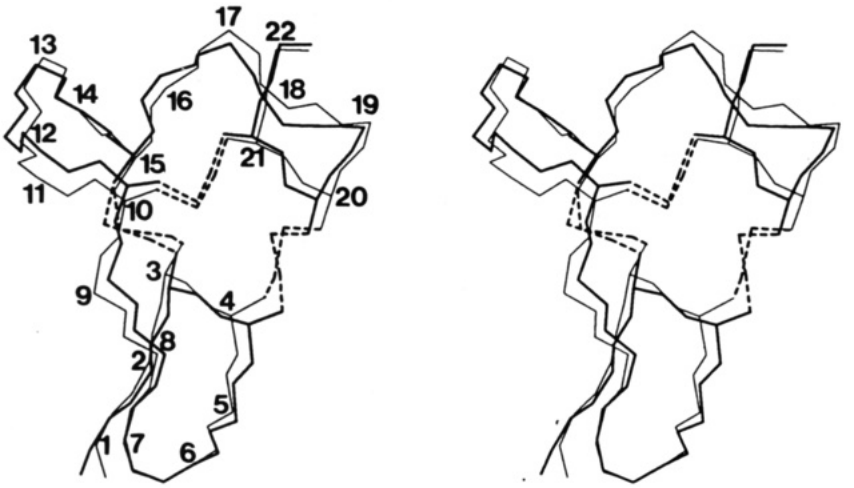

FIGURE 7: Stereoview of the best fit of the mean structure backbone of μ-conotoxin GIIIA (thin line) with that of [Ala[13]]μ-conotoxin GIIIA (bold line).

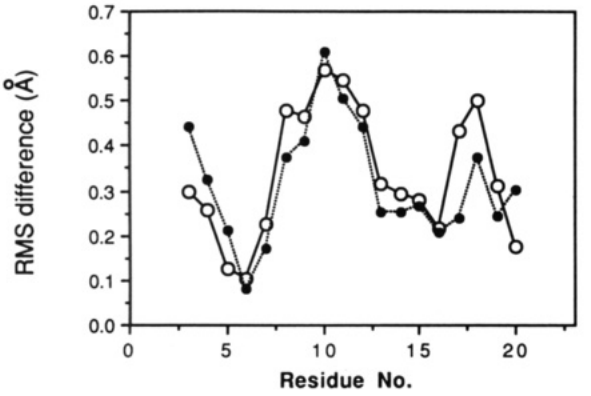

FIGURE 8: Distribution of the atomic RMS difference of 10 structures of μ-conotoxin GIIIA versus the mean structure of [Ala[13]]μ-conotoxin GIIIA (empty circles) and of 10 structures of [Ala[13]]μ-conotoxin GIIIA versus the mean structure of μ-conotoxin GIIIA (filled circles) calculated with a five-residue window.

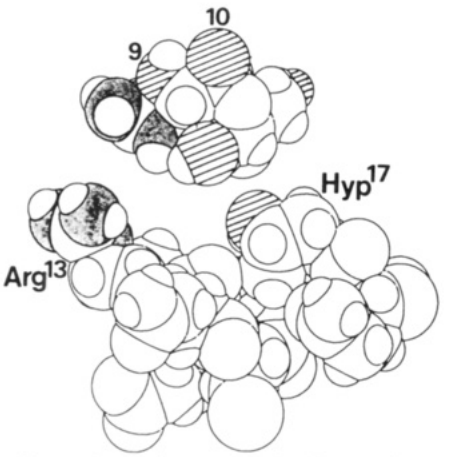

FIGURE 9: Comparison of μ-conotoxin GIIIA (bottom) with tetrodotoxin (top). Only the relevant part of a μ-conotoxin GIIIA molecule is shown. Hydroxyl oxygen atoms and guanidino nitrogen atoms are shown with cross-hatching and with shading, respectively.

calculated for each structure of native peptide versus the mean structure of Ala[13] analog and vice versa with a five-residue window (Figure 8). The maximum atomic RMS difference of 0.6 Å in the Cys[10]–Lys[11]–Asp[12] segment (Figure 8) should be regarded as an upper limit on the structural difference between the two peptides. Shifts in resonance frequenices were found to be good indices for conformation changes (Folkers et al., 1988). The small chemical shift changes in this segment (Figure 2) indicate that the structural change is small, if any.

Structure–Activity Relationships of μ-Conotoxin GIIIA. The present study revealed that the structural change associated with the inactivating substitution from Arg[13] to Ala[13] is only 0.6 Å at most in terms of the atomic RMS difference. We do not know if a conformation change of 0.6 Å can account for the 200-fold activity difference. Conformation analyses of other molecules retaining activity will answer this question. Nevertheless, we infer that the decrease in the blocking activity is due to the direct involvement of Arg[13] residue in the binding to sodium channel molecules rather than to the conformational change associated with the substitution.

Amino acid residues sensitive to replacement by an Ala residue are Arg[13] > Arg[19] > Hyp[17] > Lys[16] > Arg[1] > Lys[8] with the extent of activity loss in this order (Sato et al., 1991). Interestingly, the first four residues are clustered on one side of the toxin molecule (Figure 7). We would like to postulate that the μ-conotoxin GIIIA molecule binds to the muscle-type sodium channel with this side. Since the binding interface of the toxin molecule is rather wide [in agreement with the macrosite model of Olivera et al. (1991)], effects of one amino acid substitution will be compensated by the binding of other side chains. Hence the effects of one amino acid substitution are not so drastic as in the case of tetrodotoxin or saxitoxin. A recent finding that multiple anionic residues of the channel molecules are involved in the tetrodotoxin and saxitoxin sensitivity (Terlau et al., 1991) supports the macrosite model.

A structure–activity relationship study of tetrodotoxin and saxitoxin showed that hydroxyl groups are essential for blocking sodium channels in addition to guanidino groups (Kao & Walker, 1982; Strichartz, 1984). The hydroxyl group of Hyp[17] in μ-conotoxin GIIIA is close to the important guanidino group of Arg[13] (Figure 9), suggesting that this hydroxyl group may correspond to the essential hydroxyl groups (9-OH and 10-OH in tetrodotoxin and geminal 12-OHs in saxitoxin). In agreement, replacement of Hyp[17] with Pro[17] decreases the activity by a factor of 5 (Sato et al., 1992).

The tertiary structures of μ-conotoxin GIIIA and its inactive analog determined in this study give the basis for the further understanding of the structure–activity relationships of μ-conotoxin GIIIA and for the elucidation of the difference in the structure of muscle- and neuron-type sodium channels.

ACKNOWLEDGMENT

We are grateful to Professor Shigeyuki Yokoyama and Dr. Yutaka Muto of the University of Tokyo for the use of the Bruker AM-400 spectrometer. We thank the members of Analytical Laboratory of Mitsubishi Kasei Co. Research Center for the use of the Bruker AM-500 spectrometer.

SUPPLEMENTARY MATERIAL AVAILABLE

XPLOR input files of distance constraints for the two peptides (7 pages). Ordering information is given on any current masthead page.

REFERENCES

Bax, A., & Davis, D. G. (1985) *J. Magn. Reson. 65*, 393–402.

Bodenhausen, G., Kogler, H., & Ernst, R. R. (1984) *J. Magn. Reson. 58*, 370–388.

Brooks, B. R., Bruccoleri, R. E., Olafson, B. D., States, D. J., Swaminathan, S., & Karplus, M. (1983) *J. Comput. Chem. 4*, 187–217.

Brünger, A. T. (1990) *XPLOR software manual version 2.1*, Yale University, New Haven, CT.

Clore, G. M., Brünger, A. T., Karplus, M., & Gronenborn, A. M. (1986) *J. Mol. Biol. 191*, 523–551.

Folkers, P. J. M., Clore, G. M., Driscoll, P. C., Dodt, J., Köhler, S., & Gronenborn, A. M. (1988) *Biochemistry 28*, 2601–2617.

Gray, W. R., Olivera, B. M., & Cruz, L. J. (1988) *Annu. Rev. Biochem. 57*, 665–700.

Griesinger, C., Sørensen, O. W., & Ernst, R. R. (1985) *J. Am. Chem. Soc. 107*, 6394–6396.

Hidaka, Y., Sato, K., Nakamura, H., Ohizumi, Y., Kobayashi, J., & Shimonishi, Y. (1990) *FEBS Lett. 264*, 29–32.

Jeener, J., Meier, B. H., Bachman, P., & Ernst, R. R. (1979) *J. Chem. Phys. 71*, 4546–4553.

Kao, C. Y., & Walker, S. E. (1982) *J. Physiol. (London) 323*, 619–637.

Lancelin, J.-M., Kohda, D., Tate, S., Yanagawa, Y., Abe, T., Satake, M., & Inagaki, F. (1991) *Biochemistry 30*, 6908–6916.

Macura, S., Hyang, Y., Suter, D., & Ernst, R. R. (1981) *J. Magn. Reson. 43*, 259–281.

Nakamura, H., Kobayashi, H., Ohizumi, Y., & Hirata, Y. (1983) *Experientia 39*, 590–591.

Nilges, M., Gronenborn, A. M., Brünger, A. T., & Clore, G. M. (1988) *Protein Eng. 2*, 27–38.

Ohizumi, Y., Nakamura, H., Kobayashi, J., & Catterall, W. A. (1986) *J. Biol. Chem. 261*, 6149–6152.

Olivera, B. M., Gray, W. R., Zeikus, R., McIntosh, J. M., Varga, J., Rivier, J., de Santos, V., & Cruz, L. J. (1985) *Science 230*, 1338–1343.

Olivera, B. M., Rivier, J., Clark, C., Ramilo, C. A., Corpuz, G. P., Abogadie, F. C., Mena, E. E., Woodward, S. R., Hilliyard, D. R., & Cruz, L. J. (1990) *Science 249*, 257–263.

Olivera, B. M., Rivier, J., Scott, J. K., Hilliyard, D. R., & Cruz, L. J. (1991) *J. Biol. Chem. 266*, 22067–22070.

Ott, K. H., Becker, S., Gordon, R. D., & Rüterjans, H. (1991) *FEBS Lett. 278*, 160–166.

Plateau, P., & Guéron, M. (1982) *J. Am. Chem. Soc. 104*, 7310–7311.

Rance, M., Sørensen, O. W., Bodenhausen, G., Wagner, G., Ernst, R. R., & Wüthrich, K. (1983) *Biochem. Biophys. Res. Commun. 117*, 479–485.

Sato, S., Nakamura, H., Ohizumi, Y., Kobayashi, J., & Hirata, Y. (1983) *FEBS Lett. 155*, 277–280.

Sato, K., Ishida, Y., Wakamatsu, K., Kato, R., Honda, H., Ohizumi, Y., Nakamura, H., Ohya, M., Lancelin, J.-M., Kohda, D., & Inagaki, F. (1991) *J. Biol. Chem. 266*, 16989–16991.

Sato, K., Ishida, Y., Kato, R., Honda, H., & Wakamatsu, K. (1992) in *Peptide Chemistry 1991* (Suzuki, N., Ed.) pp 227–230, Protein Research Foundation, Osaka.

Strichartz, G. (1984) *J. Gen. Physiol. 84*, 281–305.

Terlau, H., Heinemann, S. H., Stühmer, W., Pusch, M., Conti, F., Imoto, K., & Numa, S. (1991) *FEBS Lett. 293*, 93–96.

Wüthrich, K. (1986) in *NMR of Proteins and Nucleic Acids*, Wiley, New York.

Registry No. μ-Conotoxin GIIIA, 129129-65-3.